

# Hybrid DNA–gold nanostructured materials: an *ab initio* approach

I L Garzón<sup>1</sup>, E Artacho<sup>2</sup>, M R Beltrán<sup>3</sup>, A García<sup>4</sup>, J Junquera<sup>2</sup>,  
K Michaelian<sup>1</sup>, P Ordejón<sup>5</sup>, C Rovira<sup>6</sup>, D Sánchez-Portal<sup>7</sup> and  
J M Soler<sup>2</sup>

<sup>1</sup> Instituto de Física, Universidad Nacional Autónoma de México, Apartado Postal 20-364, México DF, 01000, Mexico

<sup>2</sup> Departamento de Física de la Materia Condensada and Instituto Nicolás Cabrera, Universidad Autónoma de Madrid, E-28049 Madrid, Spain

<sup>3</sup> Instituto de Investigaciones en Materiales, Universidad Nacional Autónoma de México, Apartado Postal 70-360, México DF, 01000, Mexico

<sup>4</sup> Departamento de Física Aplicada II, Universidad del País Vasco, Apartado 644, E-48080 Bilbao, Spain

<sup>5</sup> Institut de Ciència de Materials de Barcelona (CSIC) Campus de la UAB E-08193 Bellaterra, Barcelona, Spain

<sup>6</sup> Universitat de Barcelona, Martí i Franques 1, 08028 Barcelona, Spain

<sup>7</sup> Department of Physics and Materials Research Laboratory, University of Illinois, Urbana, IL 61801, USA

Received 15 January 2001, in final form 3 April 2001

## Abstract

The controlled assembly of metal nanoparticles into macroscopic materials using DNA oligonucleotides has opened new directions of research in nanoscience and nanotechnology. Here, we describe recent *ab initio* calculations on structural and electronic properties of the subsystems forming these materials: bare and thiol-passivated gold nanoclusters, gold nanowires and fragments of DNA chains. Our results indicate that gold nanoclusters are distorted dramatically by a passivating methylthiol monolayer, that monatomic gold chains are stable in zigzag geometries and that dry acidic  $\lambda$ -DNA is a good insulator. These results provide useful insights towards the complete understanding, design and proper utilization of hybrid DNA–gold nanostructured materials.

## 1. Introduction

The synthesis of new molecular nanostructured materials bearing novel properties is one of the most active fields of current research [1]. An important contribution to this subject has been the self-assembly of two- and three-dimensional super-lattices of nanometre-diameter metal particles linked to each other by organic interconnects [2, 3]. Thiol-passivated gold nanoclusters, assembled in close-packed arrays, have shown interesting electronic transport properties, such as single-electron tunnelling at room temperature, which are expected to be useful for the development of nanoscale electronics [2, 3].

Although self-organization of nanoparticles is a powerful route to grow new materials, imperfections in the super-lattice can result from incorrect chemical recognition between the constituents. This can be a serious limitation in making nanostructured materials for electronic applications, where long-

range order is important [4]. On the other hand, biological systems are able to solve complex recognition problems. In particular, DNA transmits well defined chemical information through the pairing properties of nucleotide bases. A major advance in controlling the self-assembly of metal particles was recently achieved by using oligonucleotides to organize colloidal gold nanoclusters into super-lattices, allowing for the controlled growth of novel DNA–nanostructured materials [5, 6].

These DNA–nanoparticle hybrid materials and assemblies might not only have electrical, optical and structural properties useful in nanotechnology applications but they also hold great promise for biological diagnostics, where the nanoparticles can provide unique detection signatures [7]. Although the main mechanisms to synthesize and isolate DNA–nanostructured materials (DNA–NSM) have already been discovered, further studies to fully characterize their structural, electronic, optical, transport and other physical and chemical properties are still to be performed. This task represents a challenge for

future research in nanoscience due to the complexity of these materials, which are a complex mixture of inorganic and biological structures.

The first investigations towards a full characterization of the DNA–NSM have already begun. In the initial stage, valuable information on the properties of each subsystem, metal particles and DNA, is being obtained. These separate properties will be fundamental in understanding the behaviour of the hybrid DNA–NSM. In this direction, several studies have reported results on the properties of bare and thiol-passivated gold nanoclusters and nanowires, that constitute the building blocks of DNA–NSM. Experimental techniques such as high-resolution transmission electron microscopy (HRTEM) [8, 9], x-ray powder diffraction (XRPD) [8, 10], scanning tunnelling microscopy (STM) [8] and extended x-ray absorption fine structure (EXAFS) [11] have been used to provide structural characterization on individual thiol-passivated gold nanoclusters of different sizes, whereas HRTEM [12, 13] and STM [14] have provided information on the atomic structure and conductance of gold nanowires. Furthermore, optical spectrum measurements on the smallest gold particles (1–2 nm) have shown discrete electronic transitions indicating the existence of quantum size effects in these systems [8]. At the same time, initial studies on electronic transport in sequences of DNA bases, that provide the interconnection between the metal particles in the DNA–NSM, have appeared recently [15, 16]. The main objective of these works was to establish whether DNA is a conductor or not.

Despite the existence of sophisticated experimental tools to study gold nanostructures and DNA, several questions concerning their properties and physical behaviour remain unsolved or under debate. For example, the current approach to determine nanocluster and nanowire structures is based on the comparison between experimental images [8, 9] (HRTEM, STM) or structure factors [8, 10, 11] (XRPD, EXAFS) with those calculated from geometrical models of these nanostructures. However, the actual experimental resolution is not sufficient to resolve the broad features shown in XRPD patterns of gold nanoclusters, neither have the HRTEM images allowed for a clear discrimination of the atomic positions in gold nanowires. Similarly, recent conductivity measurements on DNA have shown very different results, generating uncertainty on the possible use of this material as a conducting biopolymer in nanostructured materials [15, 16].

Theoretical approaches based on first-principles methods, which do not depend on empirical parametrizations and have a reliable predictive power, have proven to be of great utility in providing new insights, and in complementing the experimental information on DNA–NSM. The objective of this paper is to describe recent advances obtained by our group on *ab initio* studies of bare [17–19] and thiol-passivated [20] gold nanoclusters of different sizes and gold nanowires with different atomic conformations [21], and on electronic structure calculations of fragments of DNA [22]. These studies on the separate constituents of the DNA–NSM are the starting point in their full investigation, complementing the experimental information, and answering important questions on the individual properties of each subsystem. Thus, our calculations show that the passivation

effect of methylthiol monolayers on Au<sub>38</sub> clusters is strong enough to fully distort the structure of the bare cluster [20]. We also find that gold nanowires of monatomic width are stable in zigzag geometries [21], which may explain controversial measurements in their interatomic distances [12, 13]. Finally, we have predicted, and experimentally confirmed [22], the absence of dc conductivity in  $\lambda$ -DNA under dry and acid conditions. These results constitute reliable and useful information for further investigation on the suitability of hybrid DNA–gold NSM in a variety of technological applications.

The rest of the paper is organized as follows: section 2 briefly describes some details of our methodology. In section 3 we describe recent results obtained on the properties of (i) bare and thiol-passivated gold nanoclusters, (ii) gold nanowires and (iii) DNA chains. A summary of this paper is given in section 4.

## 2. Methodology

Recent advances in first-principles electronic structure methods, based on density functional theory (DFT), are opening this approach to increasingly complex systems. Of particular importance are the so-called order- $N$  methods, in which the computational cost increases linearly with the number  $N$  of atoms in the system, as opposed to the order- $N^3$  scaling of previous methods. The above methodology, including the linear scaling facility, has been implemented in the SIESTA code [23, 24]. In this approach, the atomic forces, needed in each step of the structural optimization, are obtained by solving self-consistently the quantum mechanical Kohn–Sham equations, in the local or gradient-corrected (spin) density approximations (LDA/LSD/GGA).

We use standard norm conserving pseudopotentials [26] in their fully nonlocal form [27]. Flexible linear combinations of numerical (pseudo) atomic orbitals (PAO) are used as the basis set, allowing for multiple- $\zeta$  and polarization orbitals. In order to confine the range of the pseudoatomic basis orbitals, they are slightly excited by a common ‘energy shift’  $\delta E_{\text{PAO}}$ , and truncated at the resulting radial node [24, 28]. The basis functions and the electron density are projected onto a uniform real-space grid in order to calculate the Hartree and exchange–correlation potentials and matrix elements. The grid fineness is controlled by the ‘energy cutoff’  $E_{\text{cut}}$  of the plane waves, that can be represented in it without aliasing.

## 3. Theoretical results and discussion

### 3.1. Bare and thiol-passivated gold nanoclusters

Knowledge of the lowest-energy configuration (global minimum) and the structures of low-energy isomers (local minima) is essential in predicting many of the physical and chemical properties of nanoclusters. The case of gold clusters is especially relevant since they are the building blocks of the recently synthesized DNA–NSM [2, 3, 5, 6]. Using a many-body semi-empirical Gupta potential [29] and a genetic–sybiotic algorithm [30], we have performed global unconstrained structural optimizations for bare gold nanoclusters of different sizes [31]. This procedure allows us to obtain a distribution of low-energy structures. Some representative isomers from this distribution of minima are

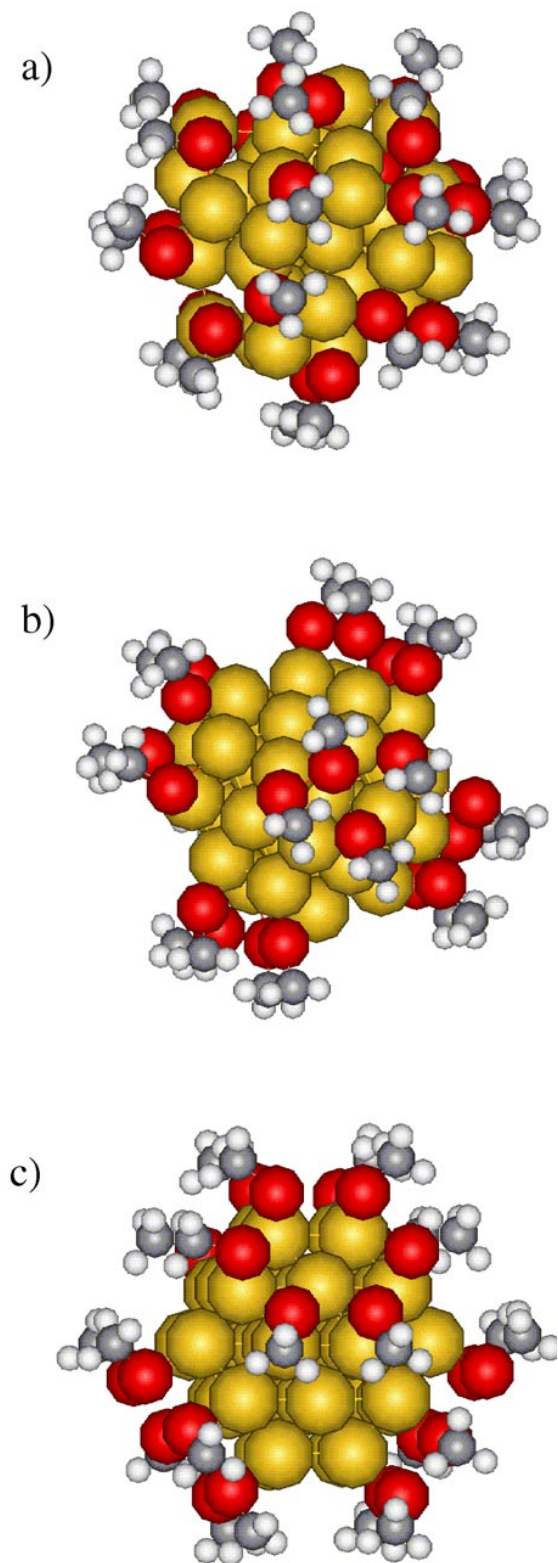


**Figure 1.** Relaxed structures of the  $\text{Au}_{38}(\text{SCH}_3)_{24}$  nanocluster. The structures were obtained starting from the cuboctahedral-fcc structure for the  $\text{Au}_{38}$  nanocrystal while the 24 thiol molecules were placed close to (a) hollow, (b) bridge and (c) top sites existing on the (100) and (111) planes of the gold cluster.

(This figure is in colour only in the electronic version, see [www.iop.org](http://www.iop.org))

used as initial configurations in the quantum mechanical structural relaxations, in order to determine the global minimum of the potential energy surface.

Our results indicate that there are many intermediate-size (1–2 nm) disordered gold nanoclusters with energy near or below the lowest-energy ordered structure [17–19, 31]. This is especially surprising since we studied ‘magic’ cluster sizes, for which very compact ordered structures exist [32]:  $\text{Au}_n$  ( $n = 38, 55, 75$ ). We have shown that the analysis of the cluster local stress can be used to understand the physical origin of the higher stability of disordered clusters with respect to their ordered isomers [19]. Specifically, it was found that the compact ordered structures are destabilized by the tendency of metallic bonds to contract at the surface, because of the decreased coordination. The cluster amorphization is also favoured by the relatively low energy associated with bond-length and coordination disorder in metals. Although these are general effects of metallic bonding, they are especially large in the case of gold [33]. The atomic disorder in the gold nanocluster structures is reflected in the broad features present in their electron density of states (DOS) as compared with the sharper structure found in the DOS corresponding to high-symmetry ordered structures [17]. Such differences could lead to distinct optical responses according to the cluster size and structural symmetry [8].

In recent HRTEM studies [34, 35] on Au and Pd nanoparticles, images of polycrystalline and amorphous structures have been reported in the size range of a few nanometres, providing experimental evidence for the existence and stability of disordered metal nanoclusters. Further experimental evidence in this direction was obtained from the excellent agreement shown between the XRPD patterns measured for  $\text{Au}_{38}$  and  $\text{Au}_{75}$  and those calculated using our disordered configurations [18, 31]. However, such comparison is not completely fair since the experimental samples corresponded to thiol-passivated gold nanoclusters, whereas the calculated structures correspond to bare gold particles. In fact, an obvious question is what the effect is of the thiol-passivating monolayer on the physical and chemical properties of gold nanoclusters.

Very recently we have performed calculations to investigate the effect of the passivation on gold nanoparticles through DFT calculations [20]. Our approach consists of performing conjugate-gradient structural relaxations starting from different cluster–monolayer configurations. Specifically, we have studied the  $\text{Au}_{38}$  cluster coated by 24 methylthiol ( $\text{SCH}_3$ ) molecules. This passivated gold cluster, with a diameter of 1.1 nm, has been isolated and characterized by XRPD and other experimental techniques [8, 10]. According to our calculations, the effect of the thiol monolayer is strong enough to distort drastically an initial cuboctahedral-fcc structure of the  $\text{Au}_{38}$  nanocrystal, with the thiol molecules symmetrically positioned on the (111) facets close to the hollow sites [20]. The relaxed structure of  $\text{Au}_{38}(\text{SCH}_3)_{24}$  corresponds to a disordered, passivated nanocluster where the sulphur atoms of the thiol heads are incorporated within the cluster surface [20]. Different patterns of charge transfer occur in this disordered, alloyed cluster surface. Figure 1(a) shows the lowest-energy configuration obtained in our structural relaxations. In figure 1(b), we show the structure obtained

by relaxing the same initial cluster geometry but with the thiol molecules symmetrically placed at the bridge sites. This structure corresponds to a local minimum  $\sim 3.5$  eV higher in energy than the isomer of figure 1(a). Interestingly, in this case we found thiol dimerization but no strong amorphization. The relaxed structure obtained starting with the thiols placed on the top sites is displayed in figure 1(c). This local minimum structure is  $\sim 5.0$  eV higher in energy than that of figure 1(a). In this case, neither thiol dimerization nor amorphization of the gold particle was found. In conclusion, these studies show strong theoretical evidence that thiol passivating molecules can strongly distort the bare geometry of gold nanoclusters. Further analysis of the different relaxed structures and their electronic properties are currently under progress.

### 3.2. Gold nanowires

Metallic nanowires show interesting quantum conductance behaviour that may be useful for nanoelectronic applications [13, 14]. They can be fabricated by elongating two metal surfaces that are in contact. The relationships between conduction, geometry and mechanical properties have been studied by simultaneous measurements of conductance [13] and applied force [14], and through direct visualization by HRTEM [12]. On the theoretical side, we have studied the structure and stability of gold monatomic nanowires through first-principles DFT calculations [21]. Our studies include results for infinite monatomic chains, using periodic boundary conditions, as well as for finite wires of various lengths, either free standing or confined between small pyramidal tips. For infinite chains that are not very stretched, the wire adopts a nonlinear, planar zigzag geometry, with two atoms per unit cell [21]. Unlike the directional covalent bonds of most chainlike molecules, metal bonds are nondirectional and lead to compact structures. However, we find that zigzag gold chains of monatomic width are (meta-) stable even as free-standing clusters, capable of holding their chainlike shape. The possibility that the observed structure could result from the directionality of a partially covalent bonding can be ruled out by the deformation density shown in figure 2. In fact, the electron density flows away from the interatomic region, becoming more delocalized along the wire. Instead, this unexpected metallic-wire stiffness, which prevents the wires from collapsing, stems from the transverse quantization in the wire, as shown in a simple free electron model [21]. We also find that the wire becomes unstable and breaks spontaneously when pulled apart beyond a maximum length of 2.9 Å, much shorter than the distance ( $\sim 3.6$  Å) apparently observed in HRTEM experiments by two different groups [12, 13]. A possible explanation of this discrepancy is that, if the actual wires observed have an odd number of atoms, with those at the extremes fixed by the contacts, the odd-numbered atoms of the zigzag structure would stay almost fixed on the same axis, while the even-numbered ones could rotate rapidly around that axis, offering a fuzzy image that could be missed in the HRTEM experiments [21]. In fact, the calculated rotation energy barrier is low enough to be overcome easily at room temperature [21].

### 3.3. DNA chains

The electron-transport properties of DNA are a subject of intense current research, since they may be important in

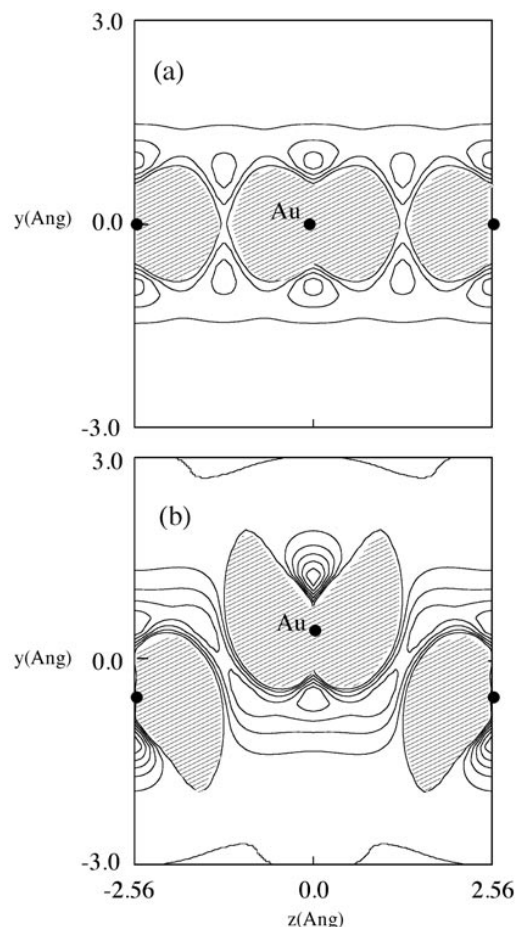


**Figure 2.** Deformation density (difference between the self-consistent electron density and the superposition of the isolated-atom densities) for (a) a linear and (b) a zigzag wire. Contour lines are shown only for positive deformation densities (lines are separated by  $10^{-3}$  e bohr $^{-3}$  beginning at zero), while the regions of charge depletion are shaded. The dots are the atomic positions.

biological processes such as radiation damage and repair [36]. Besides their biological interest, the possibility of using DNA chains as molecular wires in nanodevices has been proposed and is being explored [4]. In spite of its importance, the simple question of whether DNA is an electric conductor or not remains unsettled because of the complexity of the system and the difficulty of performing clean experiments. Experimentally, DNA conductivities differing by many orders of magnitude have been recently found [15, 16]. In one experiment, a linear  $I$ - $V$  curve was measured, finding a resistivity  $\rho \sim 10^{-4}$   $\Omega$  cm for  $\lambda$ -DNA (random sequence) molecules of 1  $\mu$ m length [15]. In another experiment, on 10 nm long freestanding poly(G)–poly(C) DNA chains, a resistivity of  $\rho \sim 10$   $\Omega$  cm was found [16]. From a theoretical point of view, it is not even clear whether DNA should conduct or not, and how the base sequence variability, and the effects of counterions and thermal vibrations, can influence the electron transport. Using order- $N$  DFT calculations within the generalized gradient approximation for exchange and correlation, we have studied an infinite chain of poly(G)–poly(C) *in vacuo*, in its dry acidic A-helix conformation [22]. The periodic unit cell has 11 base pairs and 715 atoms. After

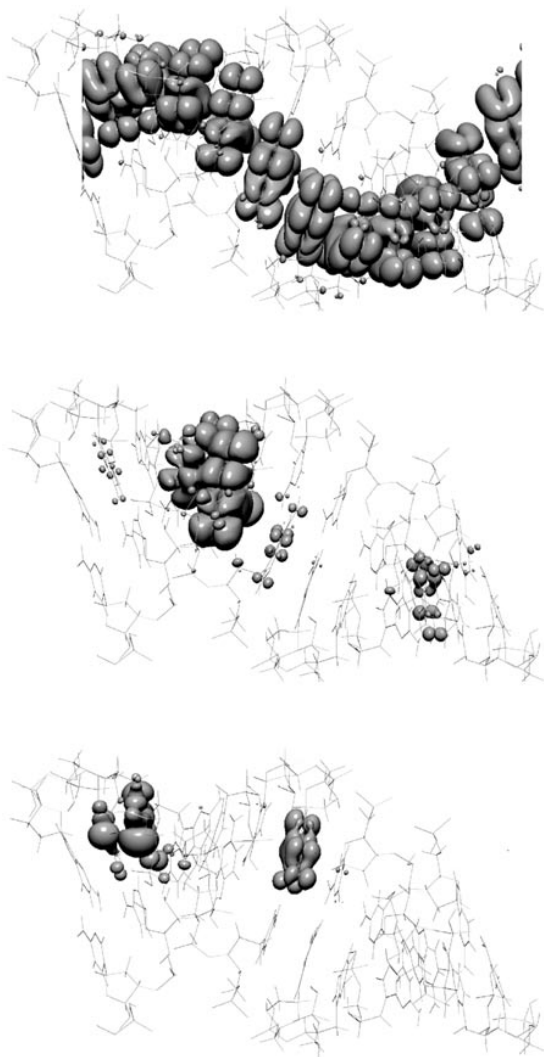


**Figure 3.** Upper panel: calculated local DOS of the relaxed DNA chain of poly(G)–poly(C), integrated over the HOMO band, which is formed by Bloch-like extended states. Middle panel: one particular HOMO state, after distorting at random the relaxed structure, with an energy increase of  $3Nk_B T$  with  $T \lesssim 300$  K. It can be seen that the electron eigenstate becomes localized in very few base pairs. Lower panel: HOMO state associated with the guanine of a swapped C–G base pair in the original sequence (the structure was relaxed again after the swapping). The density seen on the left-hand side is a non-HOMO orbital of another guanine, which resonates in energy with the HOMO of the swapped guanine, whose energy decreases considerably because of electrostatic effects.

relaxing the structure, we studied its electronic structure, finding very narrow HOMO and LUMO bands separated by an appreciable bandgap [22]. Figure 3 (upper panel) presents the local DOS integrated through the HOMO band, showing a continuous chain which could be indicative of bandlike conduction. However, even a small random distortion of the geometry dramatically changes the band structure, localizing the HOMO states (figure 3, middle panel) and scattering their energies over a range considerably larger than the original band width. After inverting one guanine–cytosine base pair per unit cell, we find an even more dramatic localization of the HOMO states, as shown in figure 3 (lower panel). These results mean that, in terms of the one-dimensional Anderson model,

the disorder fluctuations in  $\lambda$ -DNA, due to base sequence variations, are substantially larger than the bandwidth, leading to electronic localization over very few base pairs. This clearly suggests that  $\lambda$ -DNA (random sequence) chains must be strong insulators, although other conduction mechanisms (hopping) could be possible. The above prediction of the absence of dc conductivity in  $\lambda$ -DNA chains was confirmed using an experimental technique that allows measurement of conductivity through long-chain molecules [22]. In agreement with the theoretical result, an experimental lower bound of  $10^5 \Omega \text{ cm}$  for the resistivity of  $\lambda$ -DNA was found, implying that it is a very good insulator. On the other hand, it was shown that the low-energy electron bombardment used in the experiments that reported very low resistivities can induce rapid contamination and affect the conductivity measurements.

#### 4. Summary

We have described recent advances on first-principles calculations performed on the different components that constitute the newly developed DNA–gold nanostructured materials. Structural and electronic properties of bare and thiol passivated gold nanoclusters, gold nanowires and DNA chains have been calculated using DFT. The results provide important information on the physical and chemical behaviour of these subsystems. Specifically, we have shown that passivating methylthiol monolayers have a strong distorting effect on the structure of bare gold nanoclusters, that monatomic gold nanowires have stable zigzag geometries and that dc conductivity is absent from dry acidic  $\lambda$ -DNA. These results should be useful in the design and practical applications of hybrid DNA–gold nanostructures.

#### Acknowledgments

We have greatly benefited from collaborations with A Posada-Amarillas, P J de Pablo, F Moreno-Herrero, J Colchero, J Gómez-Herrero, P Herreros and A M Baró. This work was supported by Spain's Fundación Ramón Areces, and MCT grant BFM-2000-1312, and by Mexico's CONACYT grants 25083-E and 28822-E, DGAPA-UNAM grant IN101297 and the DGSCA-UNAM Supercomputing Center. We also acknowledge continued support from the Psi-k network, through the ESF Programme STRUC. DSP acknowledges support from grants US-DOE 8371494 and DEFG 02/96/ER 45439.

#### References

- [1] Whetten R L, Khoury J T, Alvarez M M, Murthy S, Vezmar I, Wang Z L, Stephens P W, Cleveland C L, Luedtke W D and Landman U 1996 *Adv. Mater.* **5** 8
- [2] Andres R P, Bein T, Dorogi M, Feng S, Henderson J I, Kubiak C P, Mahoney W, Osifchin R G and Reifenberger R 1996 *Science* **272** 1323
- [3] Andres R P, Bielefeld J D, Henderson J I, Janes D B, Kolagunta V R, Kubiak C P, Mahoney W J and Osifchin R G 1996 *Science* **273** 1690
- [4] Bethell D and Schiffrin D J 1996 *Nature* **382** 581
- [5] Mirkin C A, Letsinger R L, Mucic R C and Storhoff J J 1996 *Nature* **382** 607

- [6] Alivisatos A P, Johnsson K P, Peng X, Wilson T E, Loweth C J, Bruchez M P Jr and Schultz P G 1996 *Nature* **382** 609
- [7] Zanchet D, Micheel C M, Parak W J, Gerion D and Alivisatos A P 2001 *Nanoletters* **1** 32
- [8] Schaaff T G, Shafigullin M N, Khoury J T, Vezmar I, Whetten R L, Cullen W G, First P N, Gutiérrez-Wing C, Ascensio J and Yacamán M J 1997 *J. Phys. Chem.* **101** 7885
- [9] Zanchet D, Moreno M S and Ugarte D 1999 *Phys. Rev. Lett.* **82** 5277
- [10] Cleveland C L, Landman U, Schaaff T G, Shafigullin M N, Stephens P W and Whetten R L 1997 *Phys. Rev. Lett.* **79** 1873
- [11] Zanchet D, Tolentino H, Martins Alves M C, Alves O L and Ugarte D 2000 *Chem. Phys. Lett.* **323** 167
- [12] Ohnishi H, Kondo Y and Takayanagi K 1999 *Nature* **395** 780
- [13] Rodrigues V, Fuhrer T and Ugarte D 2000 *Phys. Rev. Lett.* **85** 4124
- [14] Rubio G, Agraït N and Vieira S 1996 *Phys. Rev. Lett.* **76** 2302
- [15] Fink H W and Schönenberger C 1999 *Nature* **398** 407
- [16] Porath D, Bezryadin A, De Vries S and Dekker C 2000 *Nature* **403** 635
- [17] Garzón I L, Michaelian K, Beltrán M R, Posada-Amarillas A, Ordejón P, Artacho E, Sánchez-Portal D and Soler J M 1998 *Phys. Rev. Lett.* **81** 1600
- [18] Garzón I L, Michaelian K, Beltrán M R, Posada-Amarillas A, Ordejón P, Artacho E, Sánchez-Portal D and Soler J M 1999 *Eur. J. Phys. D* **9** 211
- [19] Soler J M, Beltrán M R, Michaelian K, Garzón I L, Ordejón P, Sánchez-Portal D and Artacho E 2000 *Phys. Rev. B* **61** 5771
- [20] Garzón I L, Rovira C, Michaelian K, Beltrán M R, Ordejón P, Junquera J, Sánchez-Portal D, Artacho E and Soler J M 2000 *Phys. Rev. Lett.* **85** 5250
- [21] Sánchez-Portal D, Artacho E, Junquera J, Ordejón P, García A and Soler J M 1999 *Phys. Rev. Lett.* **83** 3884
- [22] de Pablo P J, Moreno-Herrero F, Colchero J, Gómez-Herrero J, Herrero P, Baró A M, Ordejón P, Soler J M and Artacho E 2000 *Phys. Rev. Lett.* **85** 4992
- [23] Ordejón P, Artacho E and Soler J M 1996 *Phys. Rev. B* **53** 10441
- Sánchez-Portal D, Ordejón P, Artacho E and Soler J M 1997 *Int. J. Quantum Chem.* **65** 453
- [24] Artacho E, Sánchez-Portal D, Ordejón P, García A and Soler J M 1999 *Phys. Status Solidi b* **215** 809
- [25] Kohn W and Sham L J 1965 *Phys. Rev.* **145** 561
- [26] Troullier N and Martins J L 1991 *Phys. Rev. B* **43** 1993
- [27] Kleinman L and Bylander D M 1982 *Phys. Rev. Lett.* **48** 1425
- [28] Sankey O F and Niklewski D J 1989 *Phys. Rev. B* **40** 3979
- [29] Rossato V, Guillope M and Legrand B 1989 *Phil. Mag. A* **59** 321
- [30] Michaelian K 1998 *Am. J. Phys.* **66** 231
- Michaelian K 1998 *Chem. Phys. Lett.* **293** 202
- [31] Michaelian K, Rendón N and Garzón I L 1999 *Phys. Rev. B* **60** 2000
- [32] Wales D J 1996 *Science* **271** 925
- [33] Garzón I L and Posada-Amarillas A 1996 *Phys. Rev. B* **54** 11796
- [34] Tehuacanero S, Herrera R, Avalos M and Yacamán M J 1992 *Acta Metall. Mater.* **40** 1663
- [35] Krakow W, Yacamán M J and Aragón J L 1994 *Phys. Rev. B* **49** 10591
- [36] Kelley S O and Barton J K 1999 *Science* **283** 385